HAL open science

Bifurcations of Transonic Flow Past Flattened Airfoils

Alexander Kuzmin

To cite this version:

Alexander Kuzmin. Bifurcations of Transonic Flow Past Flattened Airfoils. 2008. hal-00433168

HAL Id: hal-00433168

https://hal.science/hal-00433168

Preprint submitted on 18 Nov 2009

HAL is a multi-disciplinary open access archive for the deposit and dissemination of scientific research documents, whether they are published or not. The documents may come from teaching and research institutions in France or abroad, or from public or private research centers.

L'archive ouverte pluridisciplinaire **HAL**, est destinée au dépôt et à la diffusion de documents scientifiques de niveau recherche, publiés ou non, émanant des établissements d'enseignement et de recherche français ou étrangers, des laboratoires publics ou privés.

Printed version of a Keynote Lecture at the Fifth International Conference on Computational Fluid Dynamics, July 8, 2008, Seoul National University, Korea.

Bifurcations of Transonic Flow Past Flattened Airfoils

Alexander Kuz'min

St Petersburg State University, Institute of Mathematics and Mechanics,
28 University Ave., 198504 St Petersburg, Russia
alexander.kuzmin@pobox.spbu.ru

Bifurcations and non-uniqueness of the inviscid transonic flow past flattened airfoils were revealed by Jameson [1], Hafez & Guo [2], Caughey [3], and Kuzmin [4] using various Euler solvers. Turbulent flow over such airfoils may exhibit self-exciting oscillations, i.e., a buffet onset, in addition to the bifurcations [5, 6, 7].

In this paper we examine turbulent flow past a simple symmetric airfoil with a flat midpart and flow past the asymmetric J-78 airfoil designed by A. Jameson [1]. The study is focused on freestream conditions in which there exist:

- bifurcations of the entire flow structure,
- buffet onset caused by instability of the shock-induced boundary layer separation.

For the symmetric airfoil, computations show both bifurcations and buffet onset in a range of the freestream Mach number M_∞ at zero angle of attack α. For the asymmetric J-78 airfoil with a small curvature of the upper surface, instabilities of the flow structure occur at negative α.

1 Symmetric Airfoil with a Flat Midpart

We consider a smooth symmetric airfoil (see Fig. 1) whose bow and aft portions are constituted by circular arcs of radius R whereas the midpart is flat:

$$\left.\begin{aligned} y(x) &= \mp b \pm \sqrt{b^2 + a^2 - (x-a)^2}\,, && 0 \le x \le a\,, \\ y(x) &= \mp b \pm \sqrt{b^2 + a^2 - (x-1+a)^2}\,, && 1-a \le x \le 1\,, \\ y(x) &= \pm h/2\,, && a \le x \le 1-a\,. \end{aligned}\right\} \quad (1)$$

The parameter b is the distance from the circumcenter to the $x-$axis. By comparing the relations $R = (a^2 + b^2)^{1/2}$ and $R = b + h/2$, one can easily express b in terms of a and h: $b = (a^2 - h^2/4)/h$.

We specify $h = 0.09$ for the airfoil thickness and $a = 0.25$ for the beginning of the flat portion. Such an airfoil may be treated as one obtained from the well-known circular arc airfoil of thickness 18% by cutting it in half and inserting the flat midpart of the same length.

The far-field boundary Γ of a lens-type computational domain was located at distances between 40 and 100 airfoil chord lengths from the origin in the plane (x, y) (see Fig. 2). Fixed values of the angle of attack α, the Mach number M_∞ and static temperature T_∞ are given on the inflow part of Γ, whereas the static pressure p_∞ is prescribed on the outflow part of the boundary. The no-slip condition is used on the airfoil. Initial data are either a uniform flow at the given freestream Mach number M_∞ or a flow field obtained previously for other values of M_∞ and α. Solutions of the URANS equations were obtained with a finite volume solver in which the equations are discretized in space on unstructured meshes using a high resolution upwind scheme [6]. We employed the SST$-k-\omega$ turbulence model, which is known to predict the buffet onset with good accuracy [8]. Hybrid computational meshes of about $180,000$ grid points were constituted by quadrangular structured grids near the airfoil and unstructured triangular grids further. The grid points were clustered at the shock locations, in the wake, and near the airfoil. The first grid point was located at a distance of 4×10^{-6} from the airfoil to provide the condition $y^+ < 1$. The high accuracy of numerical solutions was confirmed by a mesh-independence study and also by solving a buffet problem for the 18% circular-arc airfoil and comparison with results available in the literature [8].

The freestream parameters were chosen as follows: $T_\infty = 250$ K, $p_\infty = 108,000$ N·m^{-2},

$$0.848 \leq M_\infty \leq 0.867. \tag{2}$$

The Reynolds number based on the chord length of 0.5 m and the midvalue of interval (2) is 10.9×10^6.

For $\alpha = 0$ and $M_\infty < 0.865$, computations revealed self-exciting oscillations of shock waves and separated boundary layers in the aft region. In addition, the numerical simulation demonstrated multiple solutions in the range

$$0.856 \leq M_\infty \leq 0.861 \tag{3}$$

in which realization of a certain flow field depends on initial data and the time history of freestream conditions. For example, the flow with four supersonic regions (see Fig. 3a) was obtained by solving the problem under zero angle of attack in both the initial and boundary conditions. The asymmetric flow with three local supersonic regions (see Fig. 3b) was obtained under the condition $\alpha = 0$ on the inflow part of the boundary Γ and the uniform flow at 0.1 deg incidence for initial data.

The shaded areas in Fig. 4 point out margins of the lift coefficient oscillations versus M_∞ for flow regimes with two, three, and four local supersonic regions as indicated by the sketches. It can be seen from the left shaded area that the amplitude of lift coefficient oscillations is about 0.04 in the interval of freestream Mach number $0.849 \leq M_\infty \leq 0.854$ where the solution is unique. Meanwhile the amplitude of C_L may triple if M_∞ varies in the interval $0.854 \leq M_\infty \leq 0.859$ and also α alternates providing transitions between the solutions that correspond to the upper and lower shaded domains. This means in practice that a small perturbation, e.g., a gentle breeze superposed on the free stream, may entail severe fluctuations of the aerodynamic loads on the airfoil.

Figure 5 displays margins of the lift coefficient oscillations versus the angle of attack at $M_\infty = 0.856$. The symmetric flow regime corresponds to the section $\alpha = 0$ of the middle shaded domain. It can be seen that a very small variation of the angle of attack, $|\alpha| < 0.06$ deg , produces a small perturbation of the symmetric flow which still retains four local supersonic regions. At the same time, if $|\alpha|$ exceeds 0.06 deg, then the supersonic regions abruptly coalesce on the upper or lower surface of the airfoil. The obtained asymmetric flow field persists when α is reset to zero.

Computations demonstrated that the amplitude and frequency of the lift coefficient oscillations depend on the Reynolds number insignificantly.

2 Inviscid Flow Past the J-78 Airfoil

Transonic flow past the J-78 airfoil can exhibit double supersonic regions only on the upper surface (see Fig. 6). On the lower surface, there is either a single supersonic region or purely subsonic flow. The lift coefficient $C_L(\alpha)$ calculated for several values of M_∞ is depicted in Fig. 7. The plots are actually the same as in [1] except for the discontinuities which exist at certain values of α if

$$0.772 \leq M_\infty < 1. \tag{4}$$

Physical interpretations of the discontinuities are different for the subintervals

$$0.7775 \leq M_\infty < 1 \tag{4a}$$

and

$$0.772 \leq M_\infty < 0.7775. \tag{4b}$$

In the range (4a) the jumps of C_L are caused by the instability associated with the rupture/coalescence of local supersonic regions. At the same time, in the range (4b) the discontinuities of C_L are caused by abrupt changes of shock wave and sonic line positions without changing the number of supersonic regions (instability of the second type as discussed in [4]).

For the smaller freestream Mach numbers, $M_\infty < 0.772$, the dependence of C_L on α is continuous. In this case, with increasing angle of attack, the secondary supersonic zone (located in the aft region, see Fig. 6) shrinks and eventually disappears at a distance from the major supersonic zone.

Figure 8 presents a surface illustrating the lift coefficient C_L as a function of two variables, M_∞ and α. The surface shows a slit in accordance with the discontinuity range (4).

3 Turbulent Flow Past the J-78 Airfoil

Turbulent flow computations demonstrated clear distinctions from the results obtained for inviscid flow. It can be seen from Fig. 9 that there is a total decrease of the lift coefficient in the considered ranges of M_∞ and α. This is explained by the boundary layer separation from the lower surface at $x \approx 0.55$ (see Fig. 10) which results in smaller pressure on the surface.

In addition, there is an increase of the values of M_∞ at which the plots $C_L(\alpha)$ are discontinuous:

$$0.832 \leq M_\infty < 1 \tag{5}$$

(cf. the range (4) for inviscid flow). In the subinterval $0.837 \leq M_\infty < 1$, the discontinuities are caused by the instability associated with the rupture/coalescence of supersonic regions. In the subinterval $0.832 \leq M_\infty < 0.837$, the discontinuities are due to the instability of second type mentioned above.

The plots corresponding to smaller values of the Mach number, $M_\infty < 0.832$, are continuous. Meanwhile Figure 9 shows that variations of $C_L(\alpha)$ in the vicinity of the angle $\alpha = 0.25$ deg at $M_\infty = 0.82$ are greater than the jumps of C_L in the range (5). Therefore, the freestream parameters around $M_\infty \approx 0.82$, $\alpha \approx 0.25$ deg are even more adverse for the stability of flight than the discontinuity range (5). This feature of the turbulent flow does not show up for the inviscid one.

Figure 11 presents a complex structure of the upper supersonic zone with oblique shocks obtained for $M_\infty = 0.860$ and $\alpha = -1.29 + 0$ deg, i.e., in the case of angle α approaching the value of -1.29 deg from above. When α had been approaching it from below, computations showed a double supersonic zone on the upper surface of airfoil.

Figure 12 exhibits a surface illustrating C_L as a function of two variables, M_∞ and α, for turbulent flow. In contrast to the symmetric airfoil (1), computations haven't revealed a buffet onset in the considered ranges of the freestream parameters.

4 Conclusion

For the airfoils (1) and J-78, the numerical simulation has unveiled adverse freestream conditions which trigger flow bifurcations and jumps of the lift coefficient. These phenomena are caused by the instability of closely spaced nearsonic regions or supersonic regions in a prerupture state with inner oblique shocks. For the symmetric airfoil (1) at zero angle of attack and $M_\infty < 0.865$, the simulation showed a buffet onset in addition to the bifurcations.

References

[1] Jameson, A.: Airfoils admitting non–unique solutions of the Euler equations. AIAA Paper, No. 91-1625, 1–13 (1991)

[2] Hafez, M., Guo, W.: Nonuniqueness of transonic flows. Acta Mechanica, **138**, 177–184 (1999)

[3] Caughey, D. A.: Stability of unsteady flow past airfoils exhibiting transonic non-uniqueness. CFD Journal, **13**, No. 3 (60), 427 – 438 (2004)

[4] Kuz'min, A.: Instability and bifurcation of transonic flow over airfoils. AIAA Paper, No. 2005-4800, 1–8 (2005)

[5] Hafez, M., Guo, W.: Some anomalies of numerical simulation of shock waves. Part II: effect of artificial and real viscosity. Computers and Fluids, **28**, 721–739 (1999)

[6] Kuz'min, A., Shilkin, A.: Transonic buffet over symmetric airfoils. Proc. of the Fourth Int. Conf. on CFD, Ghent, Belgium, July 10-14, 2006, Springer (to appear)

[7] Kuz'min, A.: Bifurcations and buffet of transonic flow past flattened surfaces. Computers and Fluids, **37**, http://dx.doi.org/10.1016/j.compfluid.2008.01.017 (2008)

[8] Geissler, W., Koch, S.: Adaptive airfoil. In : Sobieczky, H. (ed) Proc. IUTAM Symposium Transsonicum IV. Kluwer, Dordrecht, 303–310 (2003)

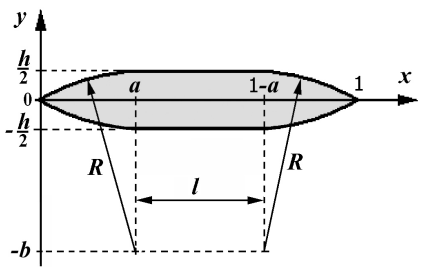

Fig. 1. The symmetric airfoil (1) under consideration: $h = 0.09,\ l = 1 - 2a = 0.5$.

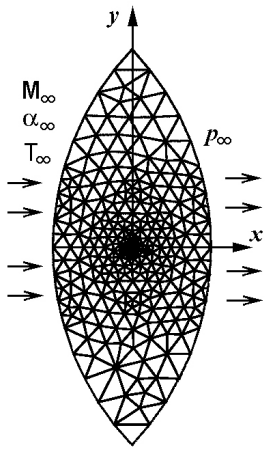

Fig. 2. A sketch of the domain and computational mesh.

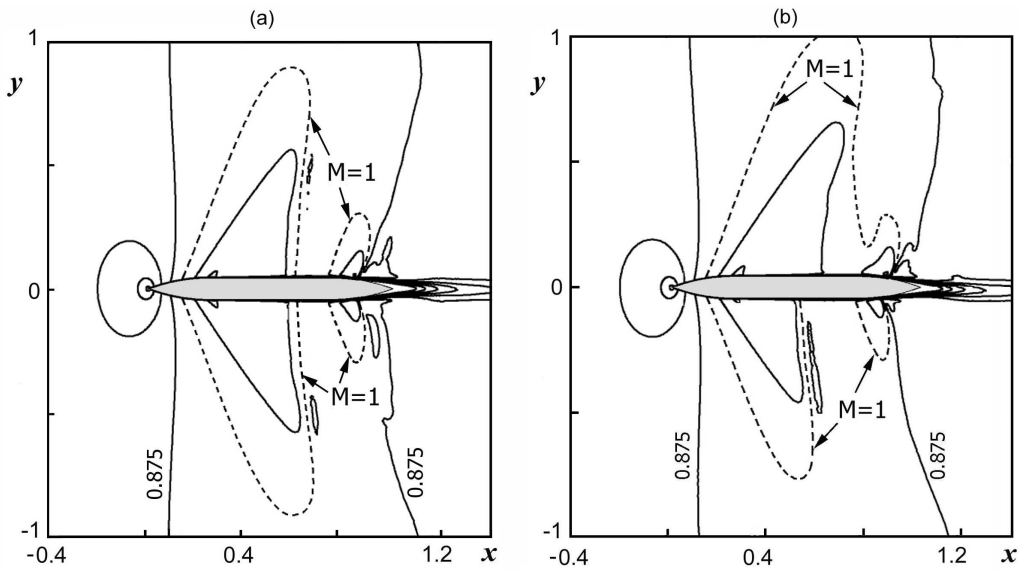

Fig. 3. Instantaneous Mach number contours at $M_\infty = 0.856$, $\alpha = 0$, $Re = 10.9 \times 10^6$ in transonic flow past the airfoil shown in Fig. 1: (a) symmetric flow with four supersonic zones, (b) asymmetric flow with three supersonic zones.

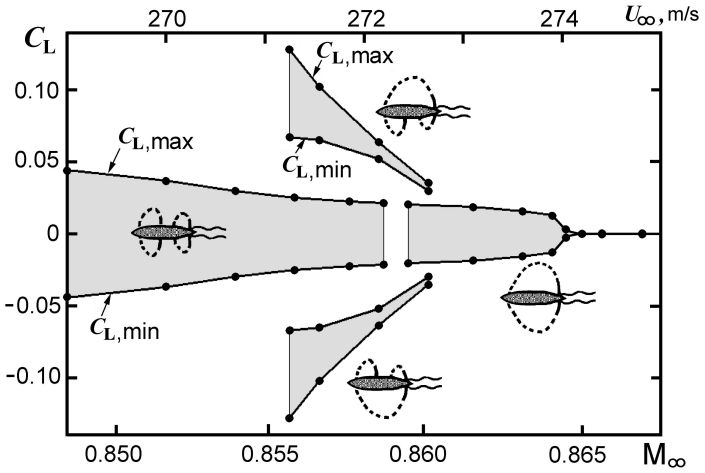

Fig. 4. Margins of the lift coefficient oscillations versus M_∞ for the airfoil (1) at $\alpha = 0,\ Re = 10.9 \times 10^6$.

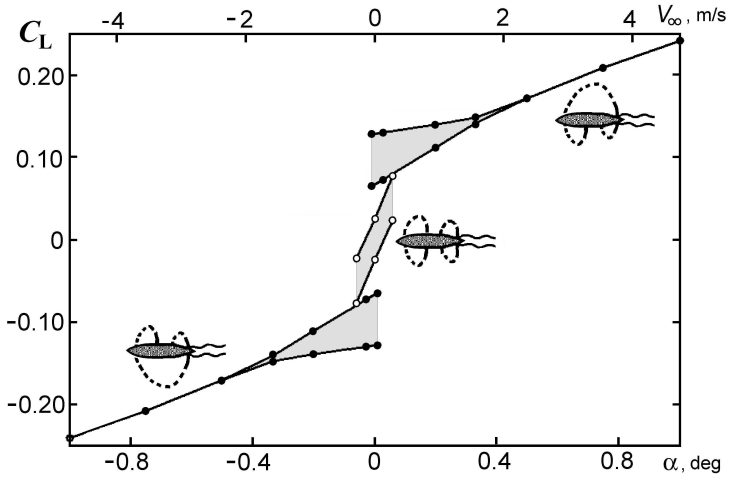

Fig. 5. Margins of the lift coefficient oscillations versus the angle of attack for the airfoil (1) at $M_\infty = 0.856,\ Re = 10.9 \times 10^6$.

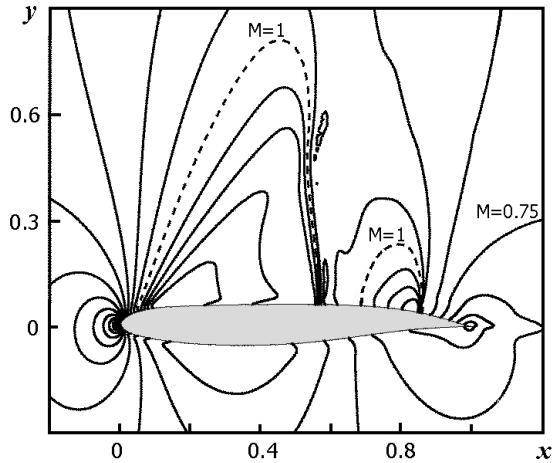

Fig. 6. Mach number contours in inviscid flow past the J-78 airfoil at $M_\infty = 0.77$, $\alpha = -0.3$ deg.

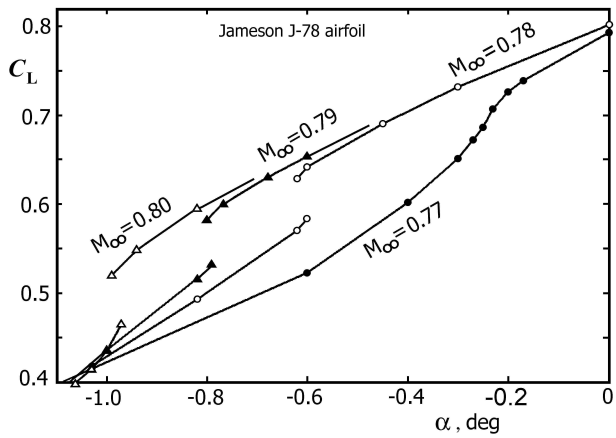

Fig. 7. Lift coefficient as a function of the angle of attack for inviscid flow past the J-78 airfoil.

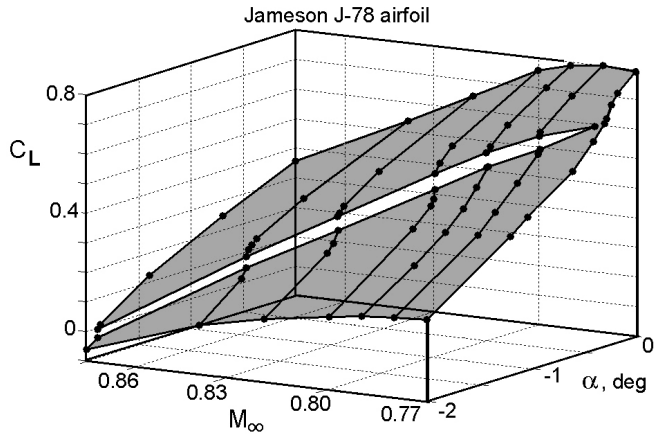

Fig. 8. Lift coefficient as a function of α and M_∞ for inviscid flow past the J-78 airfoil.

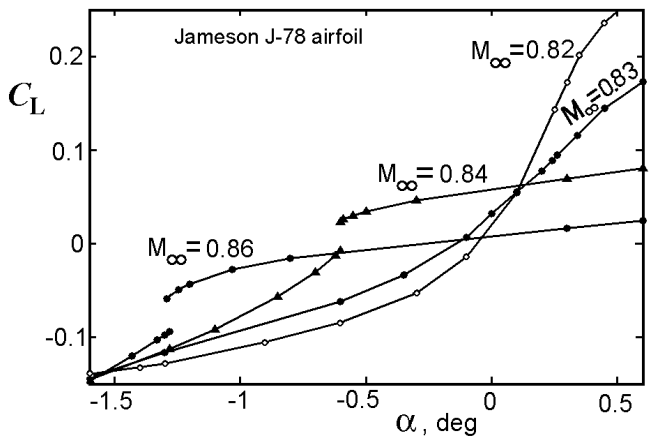

Fig. 9. Lift coefficient as a function of the angle of attack for turbulent flow past the J-78 airfoil.

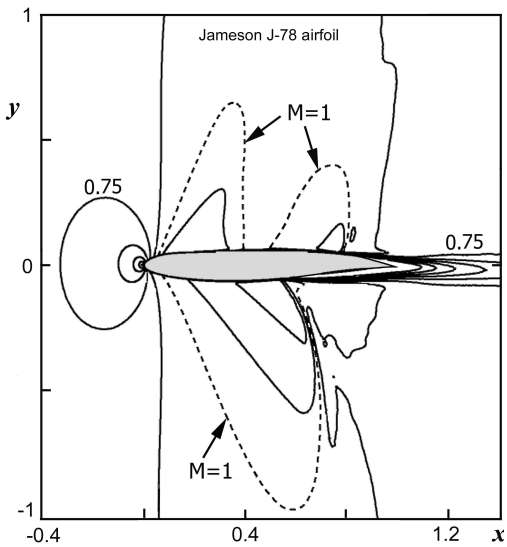

Fig. 10. Mach number contours in turbulent flow past the J-78 airfoil at $M_\infty = 0.84$, $\alpha = -0.85$ deg.

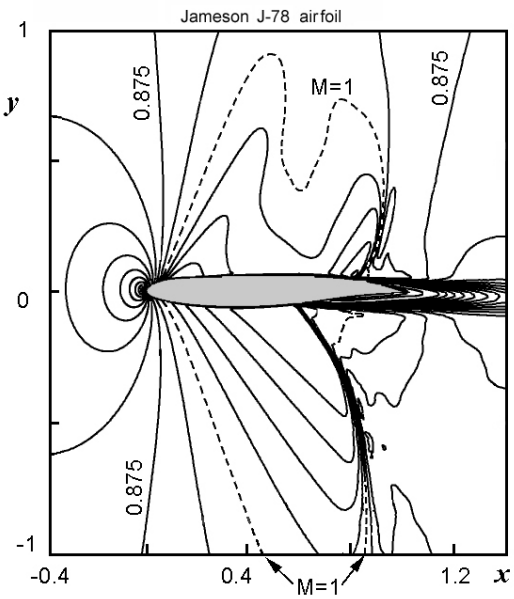

Fig. 11. Mach number contours in turbulent flow past the J-78 airfoil at $M_\infty = 0.86$, $\alpha = -1.29 + 0$ deg.

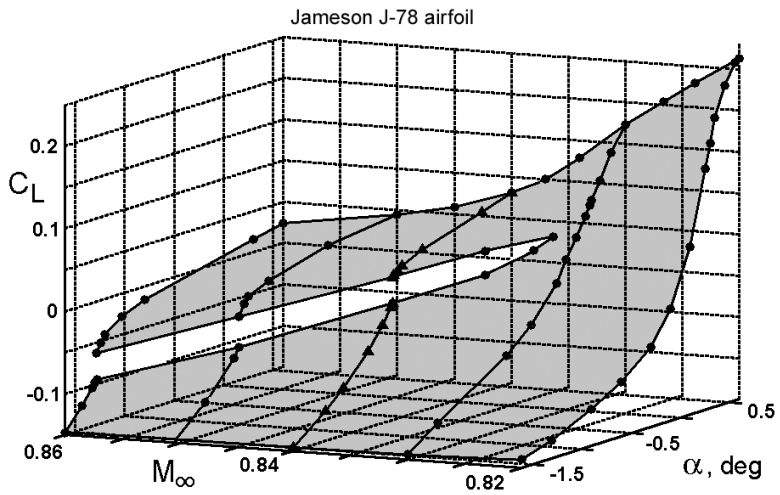

Fig. 12. Lift coefficient as a function of α and M_∞ for turbulent flow past the J-78 airfoil.